

VICTORIA UNIVERSITY
MELBOURNE AUSTRALIA

Membrane distillation and membrane electrolysis of coal seam gas reverse osmosis brine for clean water extraction and NaOH production

This is the Accepted version of the following publication

Duong, HC, Duke, Mikel, Gray, Stephen, Nelemans, B and Nghiem, LD (2016)
Membrane distillation and membrane electrolysis of coal seam gas reverse osmosis brine for clean water extraction and NaOH production. *Desalination*, 397. 108 - 115. ISSN 0011-9164

The publisher's official version can be found at
<http://www.sciencedirect.com/science/article/pii/S001191641630710X>
Note that access to this version may require subscription.

Downloaded from VU Research Repository <https://vuir.vu.edu.au/33134/>

**Membrane distillation and membrane electrolysis of coal seam gas
reverse osmosis brine for clean water extraction and NaOH production**

Revised Manuscript Submitted to

Desalination

Hung C. Duong^a, Mikel Duke^b, Stephen Gray^b, Bart Nelemans^c, Long D. Nghiem^{a,*}

^a Strategic Water Infrastructure Laboratory, School of Civil Mining and Environmental Engineering, University of Wollongong, Wollongong, NSW 2522, Australia

^b Institute for Sustainability and Innovation, College of Engineering and Science, Victoria University, P.O. Box 14428, Melbourne, Victoria, 8001, Australia

^c AquaStill, Nusterweg 69, 6136 KT Sittard, The Netherlands

* Corresponding author: Long Duc Nghiem, Email longn@uow.edu.au; Tel: +61 2 4221 4590

Abstract: Membrane distillation (MD) and membrane electrolysis (ME) were evaluated for simultaneous fresh water extraction and NaOH production from a mixture of NaCl and NaHCO₃ to simulate the composition of coal seam gas (CSG) reverse osmosis (RO) brine. Experimental results demonstrate the potential of MD for producing fresh water and simultaneously concentrating CSG RO brine prior to the ME process. MD water flux was slightly reduced by the increased feed salinity and the decomposition of bicarbonate to CO₂ during the concentration of CSG RO brine. MD operation of CSG RO brine at a concentration factor of 10 (90% water recovery) was achieved with distillate conductivity as low as 18 μS/cm, and without any observable membrane scaling. Exceeding the concentration factor of 10 could lead to deterioration in both water flux and distillate quality due to the precipitation of NaCl, NaHCO₃, and Na₂CO₃ on the membrane. With respect to ME, current density and water circulation rates exerted strong influences on the ME process performance. Combining ME with MD reduced the thermal energy requirement of ME by 3 MJ per kg of NaOH produced and the thermal energy consumption of MD by 22 MJ per m³ of clean water extracted.

Keywords: membrane distillation; membrane scaling; membrane electrolysis; sodium hydroxide production; produced water treatment; brine management.

1. Introduction

Coal seam gas (CSG) – known as coal bed methane in the US and Canada – has been recognised as an important energy source in many parts of the world. The production of CSG involves the extraction of water from underground coal seams to the surface and subsequent gas/water separation [1]. Once brought to the surface, the water is called CSG produced water [2]. CSG produced water in Australia is usually saline and highly sodic. In addition, the ionic composition of CSG produced water is dominated mostly by sodium, chloride, and bicarbonate [1, 3]. Given its saline and sodic nature, CSG produced water must be treated prior to environmental discharge or beneficial uses [1, 4].

Most current CSG produced water treatment systems utilise reverse osmosis (RO) as their core treatment process [3, 5]. Water recovery of the RO process is constrained to about 80% (5-fold concentration factor) due to the brine osmotic pressure and membrane fouling [6-8]. The brine following the RO treatment (hereafter called CSG RO brine) is highly concentrated. As a result, effective and environmentally friendly CSG RO brine management remains a significant challenge to CSG exploration.

In Australia, the dominant practice is to securely store CSG RO brine in evaporation ponds [1, 4]. All evaporation ponds for CSG RO brine storage must be constructed with two separate lining layers and an extensive monitoring system. They usually entail a security bond of about \$1 million per hectare for any future environmental clean-up. Thus, evaporation ponds are expensive and can only be a temporary option while a more cost-effective and environmentally friendly technology for CSG RO brine management is being developed [3, 4]. Indeed, extraction of usable products from CSG RO brine for beneficial uses and zero liquid discharge treatment to phase out evaporation ponds have been actively promoted by the environmental regulators [4]. A notable approach is to utilise CSG RO brine as the feed stock for sodium hydroxide (NaOH) production by membrane electrolysis (ME) [9].

ME is currently the most widely used technology by the chlor-alkali industry for NaOH production [10-12]. Compared to mercury and diaphragm cell processes, ME requires significantly less energy and poses lower environmental risk [10, 12]. As a result, ME has been used in most recent NaOH production installations [9]. The feedstock for commercial

NaOH production by ME has been sourced mostly from rock salt, concentrated salt lake brine, or concentrated seawater [9, 10]. It is also noteworthy that the feasibility of using RO brine from either CSG produced water or seawater for NaOH production by ME has been demonstrated in several recent studies [9, 10]. In addition, utilisation of CSG RO brine as the feedstock for NaOH production can be a pragmatic and innovative approach to achieve zero liquid discharge treatment of CSG produced water. This approach, however, requires further concentration of CSG RO brine to a near saturation condition [10, 13]. This step can be implemented using a thermal distillation process, such as multi-effect distillation [13, 14] or membrane distillation (MD) [15, 16].

MD is a thermally driven membrane separation process involving phase-change thermal distillation and a microporous hydrophobic membrane [17, 18]. MD retains all positive attributes of a membrane process, including modulation, compactness, and process efficiency [17, 18]. On the other hand, MD relies on a partial water vapour pressure gradient across the membrane, which is induced by a temperature difference between the feed and distillate streams, as the driving force for mass transfer. As a result, unlike RO, MD is not significantly affected by the feed solution osmotic pressure. In addition, MD can offer excellent rejection of salts and any non-volatile constituents since only water in vapour form (rather than liquid water) can be transported through the membrane. Given these attributes, MD is arguably an ideal process for the treatment of hypersaline solutions, including seawater RO brine [19], draw solution for forward osmosis treatment [20, 21], and CSG RO brine [15, 16, 22].

Several MD hybrid systems for brine concentration prior to a mineral recovery process have recently been proposed [23-25]. Chen et al. [23] employed MD for continuous concentration of NaCl brine (26.7%) prior to crystallisation. They successfully demonstrated the recovery of high quality distillate (i.e. conductivity < 10 $\mu\text{S}/\text{cm}$) and solid NaCl products. Hickenbottom and Cath [24] utilised MD to replace evaporation ponds in mineral production from hypersaline brines (i.e. > 150 g/L total dissolved solids, TDS). MD could concentrate the brines up to twofold and at many times faster than evaporation ponds while achieving near complete salt rejection [24].

CSG RO brine is usually dominated by NaHCO_3 [1, 14, 15], whose solubility is about 100 g/L and thus is significantly lower than that of NaCl [9]. Little is known about the ability of MD to further concentrate CSG RO brine prior to subsequent NaOH production by ME. In

addition, in ME, pre-heated feed brine is required for process efficiency [9, 26]. On the other hand, thermal heat is also generated by ME as a by-product of the electrolysis process. Thus, the combination of MD and ME can take advantage of the sensible heat of the MD brine, and at the same time allow for heat recovery from the ME process.

This study aims to investigate the performance of MD and ME processes for simultaneously producing fresh water and NaOH from a synthetic CSG RO brine. The effects of increased feed salinity and membrane scaling on MD water flux and distillate quality during the concentration of CSG RO brine are elucidated. Then, MD operation with CSG RO brine at high concentration factors over an extended period is demonstrated. The influences of operating conditions on ME performance, particularly its auxiliary thermal energy requirement and thermal energy co-generation with the MD brine feed, are also systematically examined.

2. Materials and methods

2.1. Materials

2.1.1. Lab-scale MD test system

A direct contact membrane distillation (DCMD) system (Fig. 1) was used. It consisted of a plate-and-frame membrane module and a flat-sheet membrane. The membrane module had two flow channels, each with depth, width, and length of 0.3, 9.5, and 35 cm, respectively. The flat-sheet membrane (Aquistill, Sittard, The Netherlands) was made of low-density polyethylene (LDPE) with nominal pore size of 0.3 μm , thickness of 76 μm , and porosity of 85%. The membrane surface area available for mass transfer inside the module was 330 cm^2 .

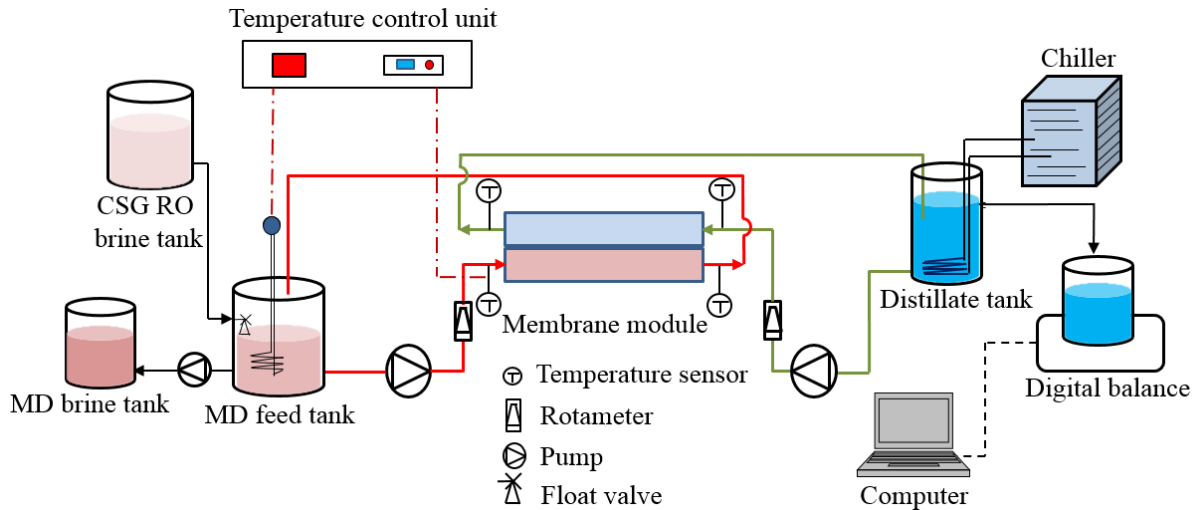


Fig. 1. Schematic diagram of the lab-scale DCMD system.

Synthetic CSG RO brine was allowed to flow into the MD feed tank by gravity via a float valve, and was heated using a heating element connected to a temperature control unit. The heated brine was circulated to the feed channel using a variable-speed gear pump (Model 120/IEC71-B14, Micropump Inc., USA). A peristaltic pump (Masterflex, John Morris Scientific Pty Ltd., Australia) was used to bleed the concentrated brine from the MD feed tank when necessary (Section 2.2). The distillate was circulated through the distillate channel using another variable-speed gear pump. The distillate temperature was regulated using a chiller (SC200-PC, Aqua Cooler, Australia) and a stainless steel heat-exchanging coil submerged directly into the distillate tank. A digital balance (PB32002-S, Mettler Toledo, Inc., USA) connected to a computer was used to weigh the excess distillate flow for determining water flux.

2.1.2. Lab-scale ME test system

The ME system consisted of a membrane module (Model E-0, AGC Engineering Ltd., Japan), a programmable power supplier (Model PSH-2018A, GW Instek, Taiwan), two peristaltic pumps (Masterflex, John Morris Scientific Pty Ltd., Australia), and a water/gas separator (Fig. 2). The membrane module was fitted with a cation exchange membrane (AGC Engineering Ltd., Japan) having a total surface area of 200 cm². The programmable power supplier was able to provide a direct current of up to 18 A (i.e. equivalent to a current density of 900 A/m²). The two peristaltic pumps circulated brine and Milli-Q water through the anode and cathode cell, respectively.

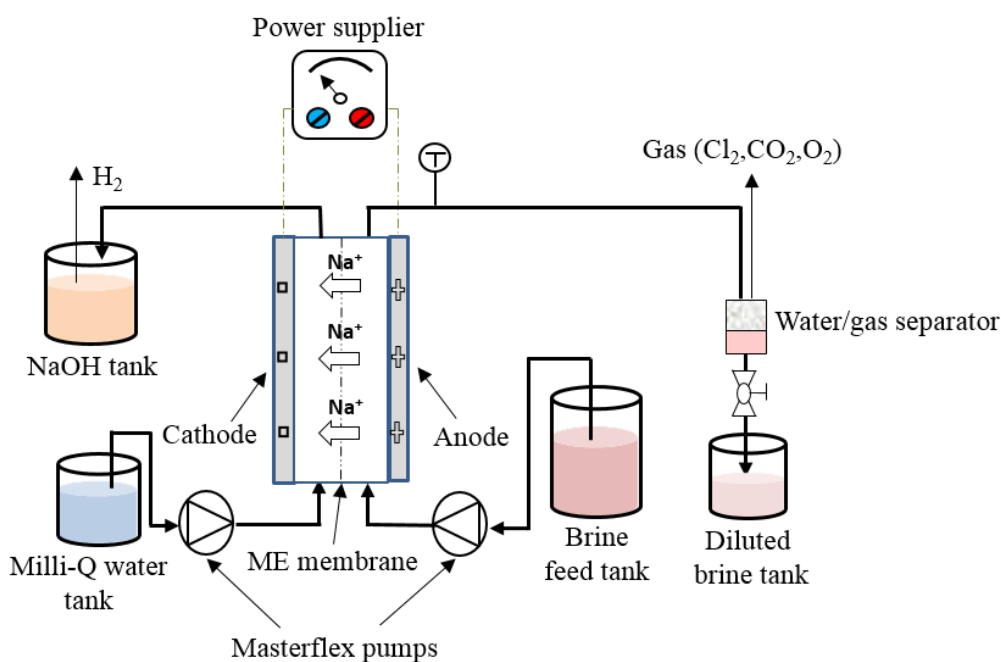


Fig. 2. Schematic diagram of the lab-scale ME system.

2.1.3. Synthetic CSG RO brine

A synthetic solution containing 10.26 g/L NaCl and 6.84 g/L NaHCO₃ (which are the two dominant salts in CSG produced water) was used to simulate CSG RO brine. This synthetic CSG RO brine had TDS, electrical conductivity, and pH of 17.1 g/L, 22.5 ± 0.2 mS/cm, and 8.2, respectively. These parameters are similar to those of the CSG RO brine obtained from a previous pilot study at the Gloucester gas field in New South Wales (Australia) [15]. In the full scale ME process for NaOH production, NaCl brine feed is first purified for removal of sparingly soluble salts [10, 13, 27]. Brine purification can be implemented before the MD treatment of CSG RO brine. Thus utilising the synthetic instead of the actual CSG RO brine does not compromise the applicability of this study.

2.2. Experimental protocols

2.2.1. DCMD operation of CSG RO brine

DCMD concentration of CSG RO brine was conducted first to ascertain the maximum concentration factor that the process could achieve before the onset of membrane scaling. Then, continuous DCMD process with the brine at high concentration factors was demonstrated. The concentrating DCMD experiments were operated at feed and distillate temperatures of 45 and 25 °C, respectively, and feed and distillate circulation rates of 1 L/min

(i.e. cross-flow velocities of 0.06 m/s). During the experiments, the volume of the feed in the MD feed tank was allowed to decrease; thus, the concentration factor of the feed increased with operating time. Water flux along with electrical conductivities of the feed and the distillate (i.e. EC_{feed} and $EC_{distillate}$, respectively) was regularly measured. Then, the system conductivity rejection (CR , %) could be calculated as:

$$CR = \left(\frac{EC_{feed} - EC_{distillate}}{EC_{feed}} \right) \times 100 \quad (1)$$

The concentration factor (CF) of the feed could be determined as:

$$CF = \frac{1}{1 - Rec} \quad (2)$$

where Rec was the system water recovery, which was a ratio between the accumulated distillate volume and the initial feed volume (i.e. 5 L).

Eight-fold concentrated synthetic CSG RO brine (136.8 g/L TDS) was used as the initial feed in the DCMD experiments at high concentration factors. The feed brine was first concentrated to a predetermined concentration factor. Then, the feed brine concentration was maintained constant by bleeding out the concentrated MD brine while allowing the synthetic CSG RO brine (17.1 g/L TDS) to flow into the MD feed tank (Fig. 2). The MD brine bled-out flow rate was determined as:

$$F_{brineout} = F_d \left(\frac{1}{Rec} - 1 \right) \quad (3)$$

where $F_{brineout}$ and F_d were the volumetric flow rates (L/h) of the bled-out brine and the produced distillate. The system water flux and conductivities of the feed and distillate were monitored. The constant concentration operation was maintained for 6 h before being terminated or switched to another concentration factor.

A new membrane was used in each DCMD experiment. At the completion of each experiment, the used membrane was air dried and stored in a desiccator for subsequent surface analyses.

The influence of feed salinity increase as a function of concentration factor on water flux could be simulated using a model previously described by Duong et al. [28]. Salinity rejection by MD was assumed to be complete. Thus, feed salinity could be readily obtained at each concentration factor value. The specific water activity (a_{water}) of the feed solution could be calculated using the Eq. 4 [29], with the assumption that NaHCO_3 and NaCl in the feed solution exerted the same influence on water activity:

$$a_{water} = 1 - 0.5x_{salt} - 10x_{salt}^2 \quad (4)$$

where x_{salt} was the total molar fraction of salts in the feed solution.

The mass transfer coefficient (K_m) of the membrane could be determined as by Duong et al. [28]. Given K_m , the system water flux at each concentration factor value could be calculated as [18]:

$$J = K_m \Delta P \quad (5)$$

where ΔP (Pa) was the partial water vapour pressure difference between the feed and the distillate streams, and was calculated as:

$$\Delta P = x_{water} a_{water} P_{feed}^0 - P_{distillate}^0 \quad (6)$$

where x_{water} was the molar fraction of water in the feed solution, P_{feed}^0 and $P_{distillate}^0$ (Pa) were the vapour pressure of pure water in the feed and the distillate, respectively. The vapour pressure of pure water could be calculated using the Antoine Equation [30]:

$$P^0 = \exp\left(23.1964 - \frac{3816.44}{T - 46.13}\right) \quad (7)$$

where T was the water temperature (K).

2.2.2. ME operation of MD brine

ME experiments with the MD brine were conducted to elucidate the influence of operating conditions on the NaOH production, desalination efficiency, and thermal energy requirement and co-generation of the process. The MD brine (at 45 °C) and Milli-Q water (at ambient temperature of 25 °C) were circulated through the anode and cathode cell,

respectively, at the same flow rates. A current density in the range from 400 to 900 A/m² was applied over anode and cathode electrodes. Under each set of operating conditions, the electrolysis process was stabilised for at least 15 min prior to measurements of the electrical conductivity and temperature of the diluted brine. Cathode effluent samples were also collected after the stabilisation for determining the process NaOH production.

The desalination capacity of the ME unit was evaluated using the reduction in concentration of the brine ($C_{reduction}$, g/L), which was calculated as:

$$C_{reduction} = \left(1 - \frac{EC_{d.brine}}{EC_{f.brine}} \right) \times C_{f.brine} \quad (8)$$

where $C_{f.brine}$ was the concentration (g/L) of the feed brine, $EC_{d.brine}$ and $EC_{f.brine}$ were the electrical conductivities of the diluted brine and the feed brine, respectively.

Specific auxiliary thermal energy requirement (α), which is the thermal energy required per mass unit of produced NaOH, was used to evaluate the auxiliary thermal energy requirement of the ME process. α (MJ/kg) was calculated as:

$$\alpha = \frac{F_{anode} \times 10^{-3} \times \rho \times C_P \times (T_{anode} - 25)}{m_{NaOH}} \quad (9)$$

where F_{anode} was the anode circulation flow rate (L/h), ρ , C_P , and T_{anode} were the density (kg/m³), specific heat capacity (MJ/kg- °C), and temperature (°C), respectively, of the ME feed brine, and m_{NaOH} was the mass flow rate of the produced NaOH (kg/h).

The ME process can also generate heat as a by-product. Thus, specific thermal energy co-generation (β) of the process was also assessed. β (MJ/kg) was calculated as:

$$\beta = \frac{F_{anode} \times 10^{-3} \times \rho \times C_P \times (T_{d.brine} - 25)}{m_{NaOH}} \quad (10)$$

where $T_{d.brine}$ was the temperature (°C) of the diluted brine leaving the anode. The calculations of ρ and C_P can be found elsewhere [31].

2.3. Analytical methods

Electrical conductivities were measured using Orion 4-Star Plus pH/conductivity meters (Thermo Scientific, Waltham, Massachusetts, USA). MD membrane surface morphology was examined using a JSM-6490LA scanning electron microscope (SEM) system (JEOL, Japan). Membrane samples were gold-coated prior to SEM analysis. X-ray diffraction (XRD) (Model MMA from GBSCI, USA) was used to determine crystals precipitated on the membrane surface at the completion of the concentrating DCMD experiments. Strength of the produced NaOH in the ME experiments was determined using the gravimetric method previously described elsewhere [9].

3. Results and discussions

3.1. DCMD treatment of CSG RO brine

3.1.1. DCMD concentration of CSG RO brine

The influence of feed salinity increase on water flux during the concentration of CSG RO brine by DCMD is shown in Fig. 3. Briefly, feed salinity increase resulted in a decrease in water activity [18, 32]. As a result, it led to a decrease in the DCMD water flux as the concentration factor increased from 1 to 11 (i.e. corresponding to increased salinity from 17.1 to 188.1 g/L) as can be seen in the simulated data in Fig. 3.

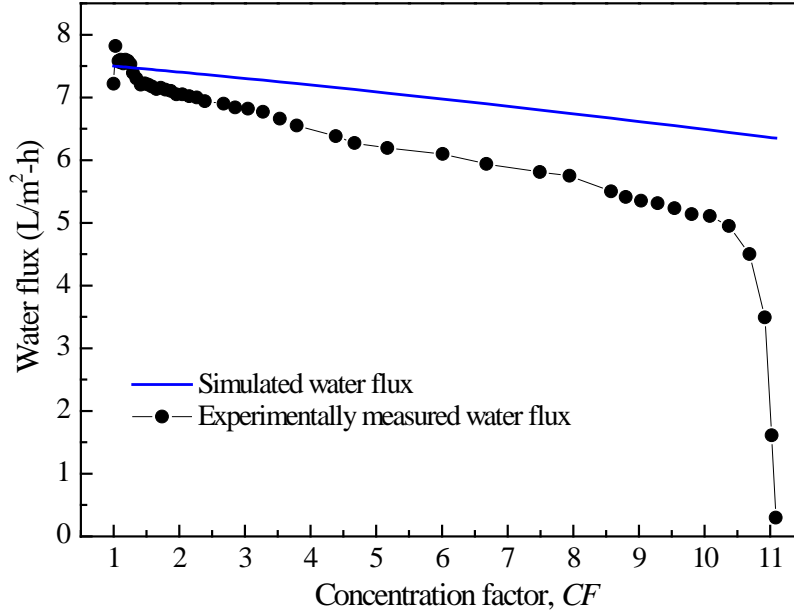


Fig. 3. Experimentally measured and simulated water flux as functions of concentration factor in the DCMD concentration of the synthetic CSG RO brine. Operating conditions: $T_{feed} = 45\text{ }^{\circ}\text{C}$, $T_{distillate} = 25\text{ }^{\circ}\text{C}$, $F_{feed} = F_{distillate} = 1\text{ L/min}$.

The experimentally measured water flux was notably lower than the simulated values based solely on water activity calculation. At concentration factor below 10, the measured water flux also linearly decreased with increasing feed salinity, but at a higher rate compared to the simulated water flux (Fig. 3). The difference between experimental and simulated values can be first attributed to the permeation of carbon dioxide (CO_2) from the feed following the decomposition of bicarbonate [15, 16, 33, 34]. CO_2 is liberated when HCO_3^- is converted to CO_3^{2-} ($2\text{HCO}_3^- \Leftrightarrow \text{CO}_3^{2-} + \text{CO}_2 + \text{H}_2\text{O}$) [34, 35], and it can compete with water vapour for their transport through membrane pores. The exclusion of concentration polarisation effect in the determination of K_m [28] is another notable factor [36, 37]. Increasing feed salinity aggravates the concentration polarisation effect in DCMD [38]; hence, the measured water flux diverged more from the simulated values at high concentration factor (Fig. 3). Finally, feed viscosity increase [34, 39], which was omitted in the model, is also responsible for the decline in the measured water flux compared to the simulated data.

It is noteworthy that the increased feed salinity together with CO₂ permeation only reduced the measured water flux by 30% when the concentration factor increased to 10. The experimentally measured water flux decreased sharply to almost zero as the concentration factor increased further from 10 to 11 (Fig. 3). At concentration factor of above 10, inorganic salts in the feed exceeded their saturation limits, precipitated on the membrane surface, and induced membrane scaling. A scaling layer was formed on the membrane, reduced the active surface for water vapour transport through the membrane [40, 41] and partial water vapour pressure on the membrane surface [42, 43], thus decreasing water flux. The scaling layer could also promote membrane wetting [44, 45]. As a result, following the occurrence of membrane scaling, the distillate conductivity increased sharply, corresponding to a remarkable decrease in conductivity rejection (Fig. 4).

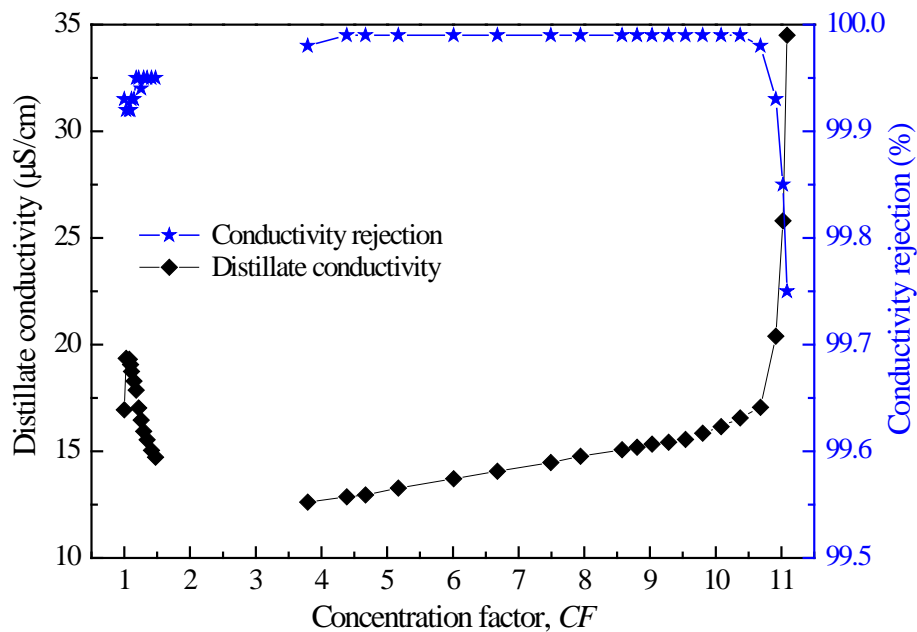


Fig. 4. Distillate conductivity and conductivity rejection as functions of concentration factor in the DCMD concentration of the synthetic CSG RO brine. Operating conditions: $T_{feed} = 45$ °C, $T_{distillate} = 25$ °C, $F_{feed} = F_{distillate} = 1$ L/min.

Microscopic analysis of the membrane surface at the end of the concentrating DCMD experiment confirmed the occurrence of membrane scaling at concentration factor exceeding 10. A layer of well-defined angular crystals was observed on the membrane surface (Fig. 5A). Furthermore, the XRD analysis of the scaled membrane (Fig. 5B) revealed the

compositions of the scaling layer of NaHCO_3 , Na_2CO_3 , and NaCl . Amongst these inorganic salts, NaHCO_3 was envisaged to be dominant given its lowest solubility [9]. The presence of Na_2CO_3 in the scale layer also confirmed the reduction of bicarbonate to CO_2 .

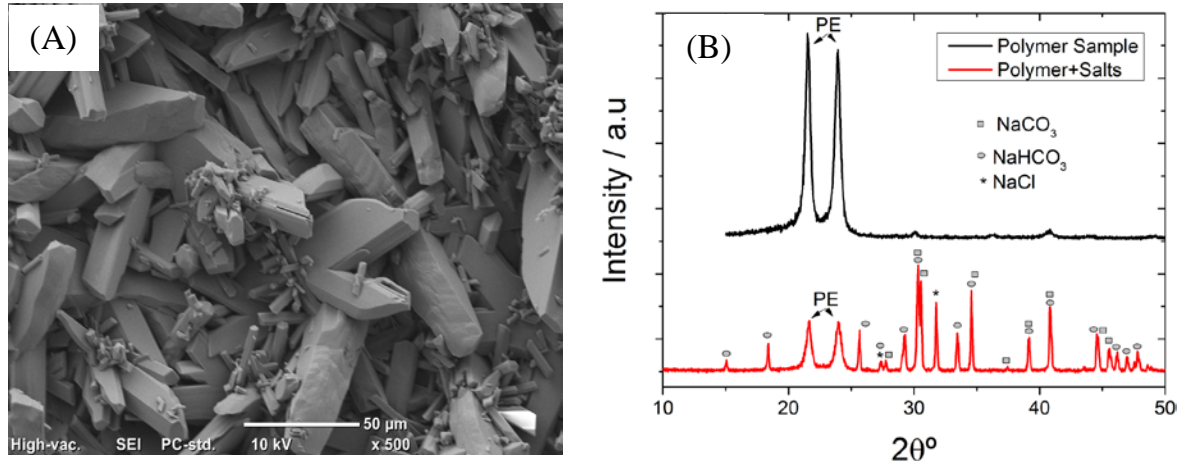


Fig. 5. (A) SEM image and (B) XRD spectra of the scaled membranes after the DCMD concentration of the synthetic CSG RO brine. DCMD operating conditions: $T_{feed} = 45\text{ }^\circ\text{C}$, $T_{distillate} = 25\text{ }^\circ\text{C}$, $F_{feed} = F_{distillate} = 1\text{ L/min}$.

The DCMD process was capable of producing distillate of high quality from the synthetic CSG RO brine concentrated up to 10-fold. The obtained distillate conductivity always remained below $20\text{ }\mu\text{S/cm}$ while the conductivity rejection was above 99.9% prior to the occurrence of membrane scaling (Fig. 4). At the beginning of the experiment, distillate conductivity slightly increased from $16\text{ }\mu\text{S/cm}$ (i.e. the conductivity of Milli-Q water used as the initial distillate) to $19\text{ }\mu\text{S/cm}$ possibly due to the transport of CO_2 from the feed to the distillate. Subsequently, it steadily decreased before slightly increasing as concentration factor approached 10 (Fig. 4). It is noteworthy that the distillate quality and the conductivity rejection obtained by the DCMD process were comparable to that of multi-effect distillation [14].

3.1.2. DCMD of CSG RO brine at high concentration factors

A stable DCMD process of the synthetic CSG RO brine at concentration factor of 10 with respects to water flux and distillate quality was achieved for over 6 h (Fig. 6). At the beginning of the process, the feed solution was concentrated from 136.8 to 171.0 g/L (i.e. concentration factor increased from 8 to 10); thus, water flux decreased from $6.5\text{ L/m}^2\text{-h}$

h due to the increase in feed salinity as previously described in section 3.1.1. The distillate conductivity increased from 16 to 26 $\mu\text{S}/\text{cm}$ because of the CO_2 permeation, which was also observed at the beginning of the concentrating DCMD experiment. For the subsequent 6 h with the constant concentration factor of 10, water flux remained stable, while the distillate conductivity steadily decreased to 18 $\mu\text{S}/\text{cm}$. The stable water flux, decreasing distillate conductivity, and the SEM analysis of the membrane surface confirmed the absence of membrane scaling at concentration factor of 10. Indeed, very few small crystals were observed on the membrane surface at the end of the DCMD experiment at the concentration factor of 10 (Fig. 7).

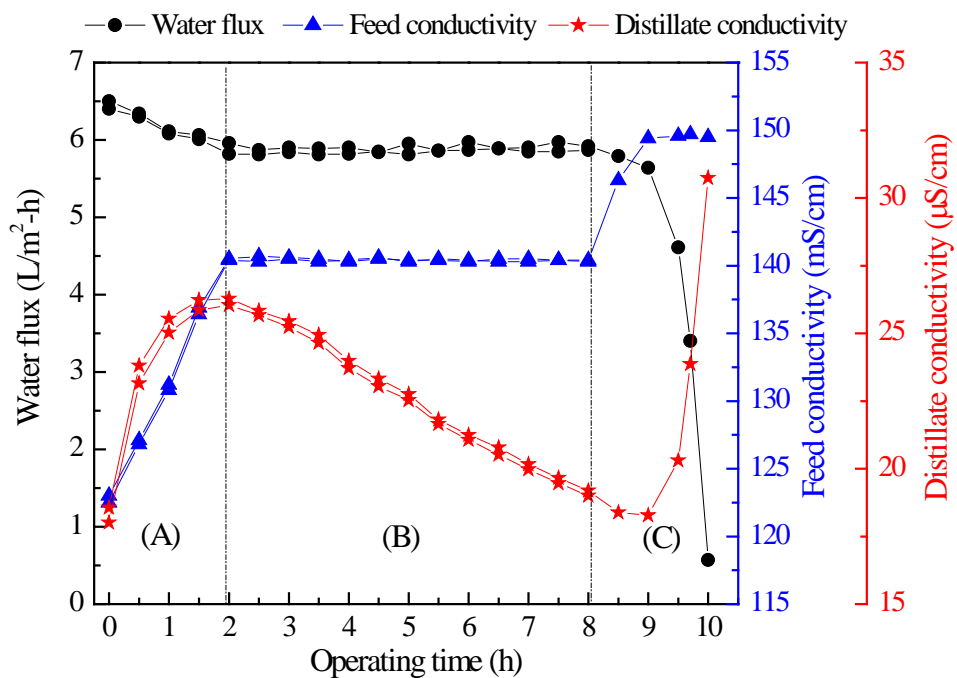


Fig. 6. Water flux, feed and distillate conductivities as functions of operating time during the DCMD of the synthetic CSG RO brine at different operation modes: (A) concentrating with concentration factor increased from 8 to 10, (B) constant concentration factor of 10, and (C) concentrating with concentration factor increased from 10 to 11. Operating conditions: $T_{feed} = 45\text{ }^{\circ}\text{C}$, $T_{distillate} = 25\text{ }^{\circ}\text{C}$, $F_{feed} = F_{distillate} = 1\text{ L}/\text{min}$.

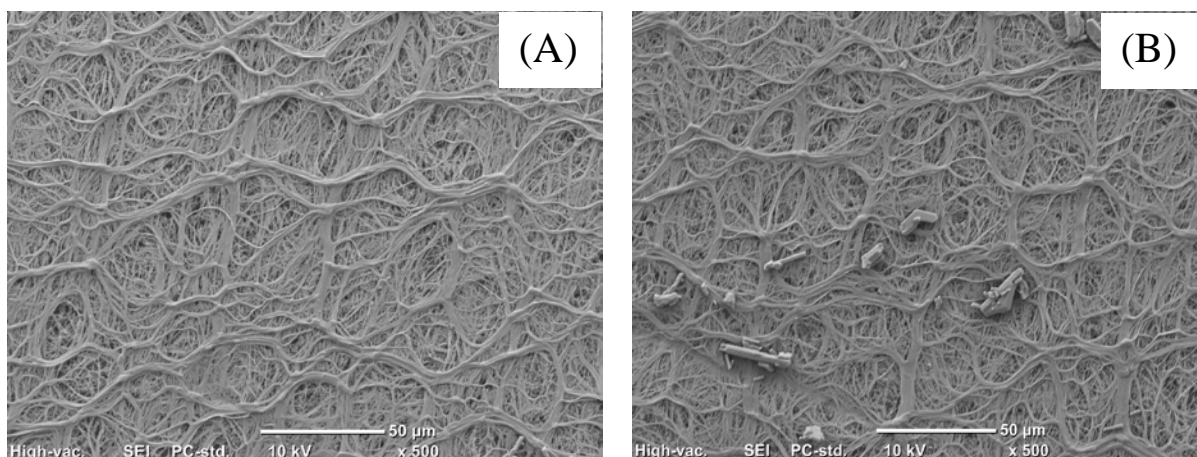


Fig. 7. SEM images of (A) a virgin membrane and (B) the membrane after 6 h DCMD treatment with the synthetic CSG RO brine at concentration factor of 10.

Operating the DCMD process with CSG RO brine at concentration factor exceeding 10 could result in scale formation on the membrane and, hence, the deterioration in the performance of the DCMD process. Membrane scaling occurred before the process reached the concentration factor of 11 (i.e. determined by monitoring the feed conductivity). Given the occurrence of membrane scaling, the system water flux decreased to almost zero while the distillate conductivity sharply increased (Fig. 6).

It is noteworthy that membrane scaling in DCMD of the synthetic CSG RO brine started at the concentration factor lower than the calculated value for the saturation point of NaHCO_3 (i.e. 11.3 at feed temperature of 45 °C [46]). This might be attributed to the temperature-proportional solubility of NaHCO_3 [46] and both concentration and temperature polarisation effects of DCMD. Concentration polarisation increases the concentration of NaHCO_3 , whereas temperature polarisation reduces the temperature of the feed (i.e. hence reducing NaHCO_3 solubility) at the membrane surface compared to the bulk feed solution, thus facilitating membrane scaling. The drop in the temperature (i.e. 4 °C) and the increase in the concentration of the brine along the feed channel (i.e. 35 cm long) could also facilitate the onset of membrane scaling. This effect is signified for pilot or large-scale MD processes, where membrane modules having much longer feed channels are employed [47-49].

Results reported in Fig. 6 demonstrate the feasibility of MD for producing fresh water and simultaneously concentrating CSG RO brine prior to the ME process for NaOH production. A stable DCMD operation of the synthetic CSG RO brine at 90% water recovery (i.e.

concentration factor of 10) without any observable membrane scaling was achieved. Given 75% water recovery of the RO process [15], the combined treatment chain UF/RO/MD (i.e. including brine purification prior to MD) can extract 97.5% fresh water from the CSG produced water. The concentrated brine following the MD process, which is only 2.5% of the initial volume of CSG produced water, can be fed to ME for the production of NaOH.

3.2. ME treatment of MD brine for NaOH production

3.2.1. Influence of current density on the performance of the ME system

Current density exerted a strong influence on the performance of the ME process with the MD brine. Elevating current density accelerated the movement of ions to the electrodes and boosted the electrolysis, hence increasing both the process NaOH production and desalination efficiency (i.e. represented by the reduction in brine concentration) (Fig. 8). At current density of 900 A/m^2 , the single-pass ME process could produce a NaOH solution of 1.15 M (4.6% w/w), and desalinate 75 g/L of salts from the MD brine feed. These obtained values are higher than those reported by Simon et al. [9] under the same operating conditions (i.e. current density and circulation flow rates). It is noted that the current study used the feed brine at a higher temperature and concentration compared to those in Simon et al. [9], thus achieving a higher process efficiency than previously reported values [9, 26].

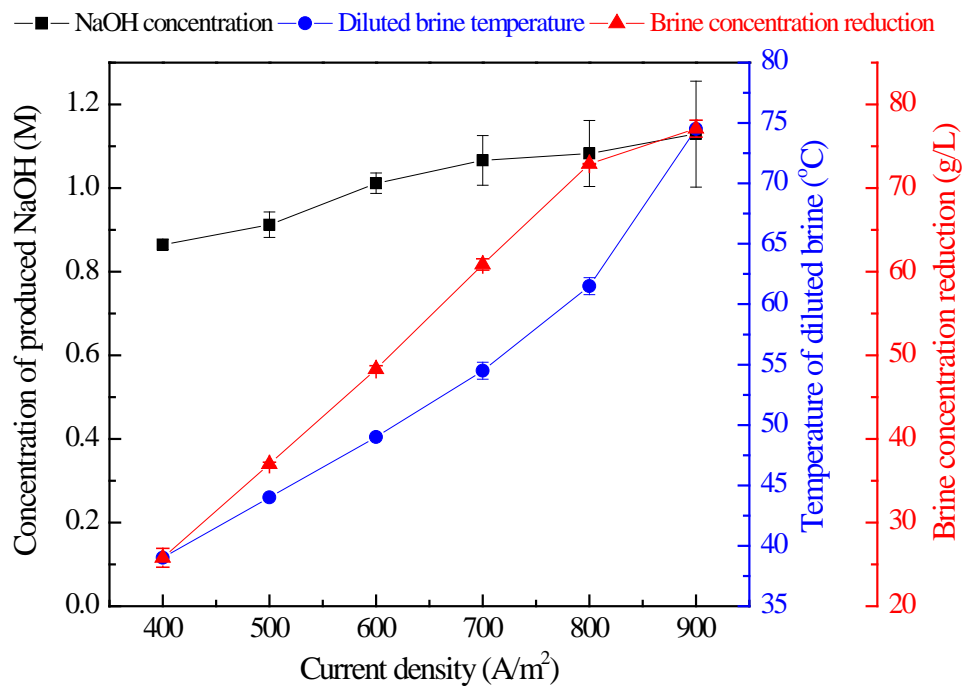


Fig. 8. Produced NaOH concentration, diluted brine temperature, and brine concentration reduction as functions of current density in the ME process of the MD brine. Operating conditions: cathode temperature $T_{cathode} = 25$ °C, anode temperature $T_{anode} = 45$ °C, anode and cathode circulation flow rates = 0.4 L/h (cross-flow velocities of 5×10^{-4} m/s). Error bars represent the standard deviation of duplicate experiments.

Elevating current density also increased the temperature of the diluted brine (Fig. 8). As reported by Simon et al. [9], the current efficiency of the ME test unit was about 50% in the investigated current density range, meaning that half of the supplied energy was converted into heat. At a low current density, the generated heat was smaller than the heat loss to the cathode; thus, the temperature of diluted brine was lower than the brine feed temperature (i.e. 45 °C). At current densities above 600 A/m², the generated heat outweighed the heat loss, thus heating the diluted brine. The diluted brine temperature nearly reached the maximum allowable operating temperature of the ME process (i.e. 80 °C) at current density of 900 A/m².

3.2.2. *Influence of circulation flow rates on the performance of the ME system*

Unlike current density, increasing anode and cathode circulation flow rates reduced the process NaOH production and desalination efficiency (Fig. 9). When circulation flow rates increased from 0.30 to 0.85 L/h (i.e. cross-flow velocity increased from 3.75×10^{-4} to 6.25×10^{-4} m/s), the concentration of produced NaOH and the reduction in brine concentration decreased from 1.40 to 0.65 M and 75 to 15 g/L, respectively. Shortened brine retention time inside the electrolyser resulted from increasing circulation flow rates can be attributed for these reductions. Shortening the brine retention time also reduced the heat loss from the anode to the cathode. As a result, the diluted brine temperature rose with increased circulation flow rates. However, the influence of circulation flow rates on diluted brine temperature was not as strong as that of current density. At the highest investigated circulation flow rate, the diluted brine temperature was well below the maximum limit (i.e. 55 compared to 80 °C).

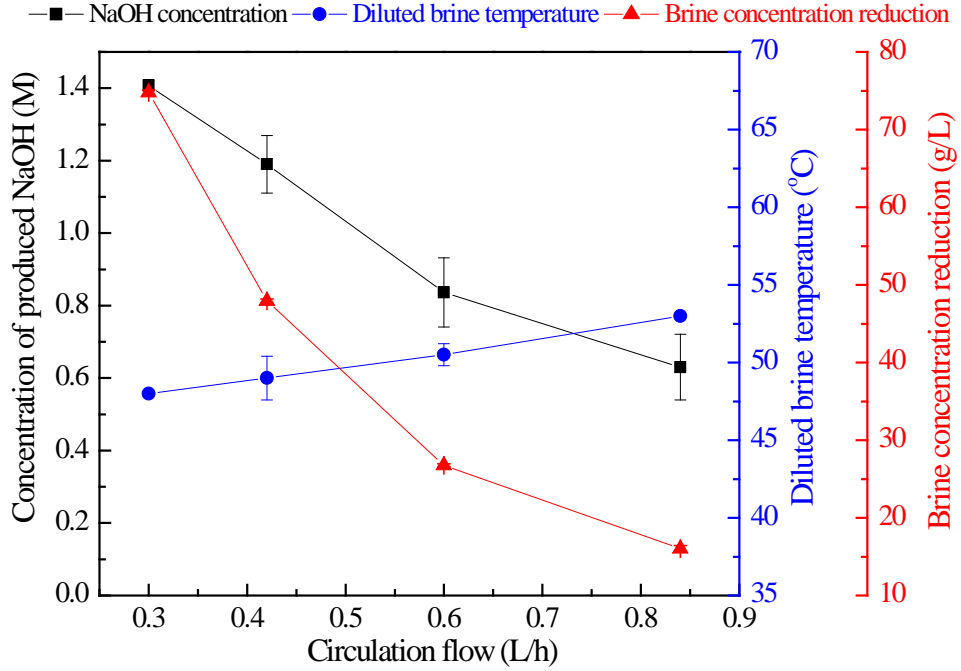


Fig. 9. Produced NaOH concentration, diluted brine temperature, and brine concentration reduction as functions of circulation flow rates in the ME process of the MD brine. Operating conditions: cathode temperature $T_{cathode} = 25$ °C, anode temperature $T_{anode} = 45$ °C; current density 600 A/m². Error bars represent standard deviation of duplicate experiments.

3.2.3. Auxiliary thermal energy requirement and co-generation by ME

The influences of current density and circulation flow rates on the specific auxiliary thermal energy requirement (α) and specific thermal energy co-generation (β) of the ME process with the MD brine are shown in Fig. 10. Increasing current density increased the NaOH production, whereas the auxiliary thermal energy required by the process remained unchanged, thus leading to a decrease in α (Fig. 10A). On the other hand, increasing current density raised the diluted brine temperature at a higher rate compared to the NaOH production. As a result, β of the process increased with current density. At current density above 500 A/m², β outweighed α . In other words, the ME process generated heat as a by-product. It is noteworthy that this generated heat (i.e. at temperature below 75 °C) can be utilised only by MD but not a conventional thermal distillation process.

Elevating circulation flow rates also resulted in an increase in β (Fig. 10B). However, unlike current density, elevating circulation flow rates reduced the NaOH production but

increased the auxiliary thermal energy demand of the process; hence, it increased α of the process.

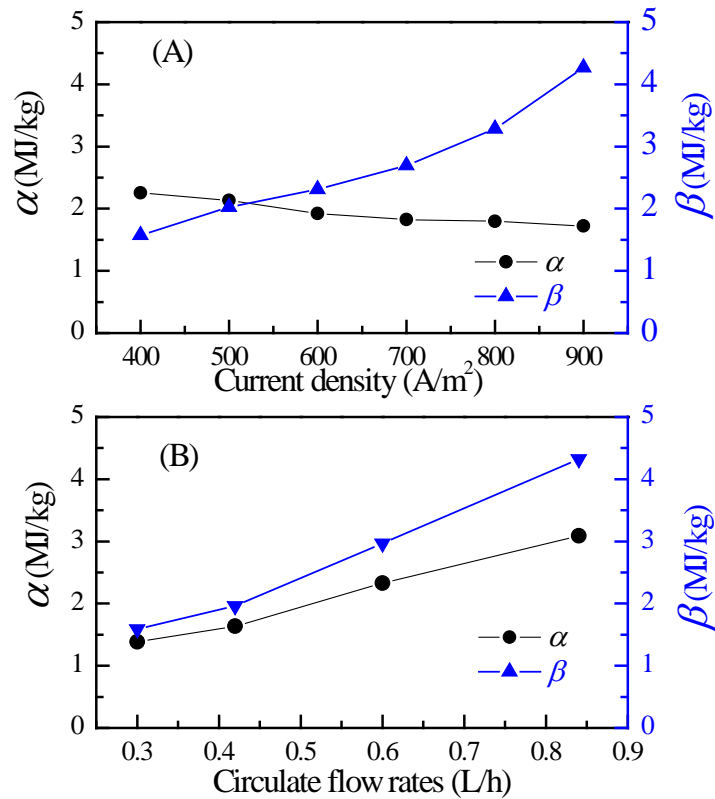


Fig. 10. Specific auxiliary thermal energy requirement (α) and specific thermal energy cogeneration (β) as functions of (A) current density (other operating conditions: cathode temperature $T_{cathode} = 25$ °C, anode temperature $T_{anode} = 45$ °C, anode and cathode circulation flow rates = 0.4 L/h), and (B) circulation flow rates (other operating conditions: cathode temperature $T_{cathode} = 25$ °C, anode temperature $T_{anode} = 45$ °C, current density 600 A/m^2) in the ME treatment the MD brine.

The results reported here show that current density and circulation flow rates are key parameters for process optimisation when integrating MD and ME for NaOH production from CSG RO brine. Complementary operating conditions between MD and ME can be achieved to avoid unnecessary heating of the feed and excessive heat production from ME. At the operating conditions used in this study, using the MD brine directly to the ME process results in 3 MJ in thermal energy saving per 1 kg of NaOH produced. Moreover, our calculation also reveals that returning the heated diluted ME brine to the MD process can reduce the MD thermal energy consumption by 22 MJ per 1 m^3 of fresh water extracted.

Further economic optimisation is required in order to ascertain the optimum ME operating conditions for a combined MD–ME process.

4. Conclusions

The treatment of CSG RO brine for beneficial reuses using MD and ME was investigated. The results demonstrate significant benefits of combining MD and ME for simultaneous clean water extraction and NaOH production from CSG RO brine. Increased feed salinity and the reduction of bicarbonate to CO₂ during MD concentration of CSG RO brine only resulted in a slight decline in water flux. MD operation of the 10-fold concentrated CSG RO brine (i.e. 90% water recovery) was achieved for over an extended period with distillate of superior quality and without any membrane scaling. At the concentration factor of above 10 folds, the precipitation of NaCl, NaHCO₃, and Na₂CO₃ on the membrane was observed together with a severe decline in water flux and distillate quality. With respect to the ME process, current density and circulation flow rates could exert strong influences on the NaOH production efficiency. By combining ME with MD for NaOH production from CSG RO brine, thermal energy savings could be achieved for both processes (i.e. 3 MJ per 1 kg of NaOH produced by ME and 22 MJ per 1 m³ of fresh water extracted by MD).

References

- [1] L.D. Nghiem, T. Ren, N. Aziz, I. Porter, and G. Regmi, Treatment of coal seam gas produced water for beneficial use in Australia: A review of best practices, *Desalin. Water Treat.* 32 (2011) 316-323.
- [2] R.M. Abousnina, L.D. Nghiem, and J. Bundschuh, Comparison between oily and coal seam gas produced water with respect to quantity, characteristics and treatment technologies: a review, *Desalin. Water Treat.* 54 (2015) 1793-1808.
- [3] M. Zaman, G. Birkett, C. Pratt, B. Stuart, and S. Pratt, Downstream processing of reverse osmosis brine: Characterisation of potential scaling compounds, *Water Res.* 80 (2015) 227-234.
- [4] State of Queensland (Department of Environment and Heritage Protection), Coal seam gas water management policy, Brisbane, 2012, 1-6.
- [5] G.J. Millar, J. Lin, A. Arshad, and S.J. Couperthwaite, Evaluation of electrocoagulation for the pre-treatment of coal seam water, *J. Water Pro. Eng.* 4 (2014) 166-178.

- [6] P. Xu and J.E. Drewes, Viability of nanofiltration and ultra-low pressure reverse osmosis membranes for multi-beneficial use of methane produced water, *Sep. Purif. Technol.* 52 (2006) 67-76.
- [7] S. Mondal and S.R. Wickramasinghe, Produced water treatment by nanofiltration and reverse osmosis membranes, *J. Membr. Sci.* 322 (2008) 162-170.
- [8] J.E. Drewes, N.T. Hancock, K.L. Benko, K. Dahm, P. Xu, D. Heil, and T.Y. Cath, Treatment of coalbed methane produced water, *Explor. Prod. Oil Gas Rev.* 7 (2009) 126-128.
- [9] A. Simon, T. Fujioka, W.E. Price, and L.D. Nghiem, Sodium hydroxide production from sodium carbonate and bicarbonate solutions using membrane electrolysis: A feasibility study, *Sep. Purif. Technol.* 127 (2014) 70-76.
- [10] N. Melián-Martel, J.J. Sadhwani, and S. Ovidio Pérez Báez, Saline waste disposal reuse for desalination plants for the chlor-alkali industry: The particular case of pozo izquierdo SWRO desalination plant, *Desalination* 281 (2011) 35-41.
- [11] A.A. Jalali, F. Mohammadi, and S.N. Ashrafizadeh, Effects of process conditions on cell voltage, current efficiency and voltage balance of a chlor-alkali membrane cell, *Desalination* 237 (2009) 126-139.
- [12] S. Savari, S. Sachdeva, and A. Kumar, Electrolysis of sodium chloride using composite poly(styrene-co-divinylbenzene) cation exchange membranes, *J. Membr. Sci.* 310 (2008) 246-261.
- [13] N. Melián-Martel, J.J. Sadhwani Alonso, and S.O. Pérez Báez, Reuse and management of brine in sustainable SWRO desalination plants, *Desalin. Water Treat.* 51 (2013) 560-566.
- [14] L.D. Nghiem, C. Elters, A. Simon, T. Tatsuya, and W. Price, Coal seam gas produced water treatment by ultrafiltration, reverse osmosis and multi-effect distillation: A pilot study, *Sep. Purif. Technol.* 146 (2015) 94-100.
- [15] H.C. Duong, A.R. Chivas, B. Nelemans, M. Duke, S. Gray, T.Y. Cath, and L.D. Nghiem, Treatment of RO brine from CSG produced water by spiral-wound air gap membrane distillation - A pilot study, *Desalination* 366 (2015) 121-129.
- [16] H.C. Duong, M. Duke, S. Gray, T.Y. Cath, and L.D. Nghiem, Scaling control during membrane distillation of coal seam gas reverse osmosis brine, *J. Membr. Sci.* 493 (2015) 673-682.
- [17] E. Drioli, A. Ali, and F. Macedonio, Membrane distillation: Recent developments and perspectives, *Desalination* 356 (2015) 56-84.
- [18] A. Alkudhiri, N. Darwish, and N. Hilal, Membrane distillation: A comprehensive review, *Desalination* 287 (2012) 2-18.
- [19] J.-P. Mericq, S. Laborie, and C. Cabassud, Vacuum membrane distillation of seawater reverse osmosis brines, *Water Res.* 44 (2010) 5260-5273.

- [20] X.M. Li, B. Zhao, Z. Wang, M. Xie, J. Song, L.D. Nghiem, T. He, C. Yang, C. Li, and G. Chen, Water reclamation from shale gas drilling flow-back fluid using a novel forward osmosis-vacuum membrane distillation hybrid system, *Water Sci. Technol.* 69 (2014) 1036-1044.
- [21] M. Xie, L.D. Nghiem, W.E. Price, and M. Elimelech, A Forward Osmosis–Membrane Distillation Hybrid Process for Direct Sewer Mining: System Performance and Limitations, *Environ. Sci. Technol.* 47 (2013) 13486-13493.
- [22] D.L. Shaffer, L.H. Arias Chavez, M. Ben-Sasson, S. Romero-Vargas Castrillón, N.Y. Yip, and M. Elimelech, Desalination and Reuse of High-Salinity Shale Gas Produced Water: Drivers, Technologies, and Future Directions, *Environ. Sci. Technol.* 47 (2013) 9569-9583.
- [23] G. Chen, Y. Lu, W.B. Krantz, R. Wang, and A.G. Fane, Optimization of operating conditions for a continuous membrane distillation crystallization process with zero salty water discharge, *J. Membr. Sci.* 450 (2014) 1-11.
- [24] K.L. Hickenbottom and T.Y. Cath, Sustainable operation of membrane distillation for enhancement of mineral recovery from hypersaline solutions, *J. Membr. Sci.* 454 (2014) 426-435.
- [25] N. Ghaffour, J. Bundschuh, H. Mahmoudi, and M.F.A. Goosen, Renewable energy-driven desalination technologies: A comprehensive review on challenges and potential applications of integrated systems, *Desalination* 356 (2015) 94-114.
- [26] S.P. Nunes and K.-V. Peinemann, *Membrane technology in the chemical industry*, Wiley-VCH Verlag GmbH, 2001, 251-258.
- [27] S.S. Madaeni and V. Kazemi, Treatment of saturated brine in chlor-alkali process using membranes, *Sep. Purif. Technol.* 61 (2008) 68-74.
- [28] H.C. Duong, P. Cooper, B. Nelemans, and L.D. Nghiem, Optimising thermal efficiency of direct contact membrane distillation via brine recycling for small-scale seawater desalination, *Desalination* 374 (2015) 1-9.
- [29] R.W. Schofield, *Membrane distillation: An experimental study*, Doctor of Philosophy, The University of New South Wales, 1989.
- [30] R.C. Reid, J.M. Prausnitz, and T.K. Shewood, *The Properties of Gases and Liquids*, McGraw-Hill, New York, 1977.
- [31] H.T. El-Dessouky and H.M. Ettouney, *Fundamentals of Salt Water Desalination*, Elsevier Science B.V., The Netherlands, 2002, 526-563.
- [32] K.W. Lawson and D.R. Lloyd, Membrane distillation, *J. Membr. Sci.* 124 (1997) 1-25.
- [33] M. Gryta, Alkaline scaling in the membrane distillation process, *Desalination* 228 (2008) 128-134.

- [34] P. Zhang, P. Knötig, S. Gray, and M. Duke, Scale reduction and cleaning techniques during direct contact membrane distillation of seawater reverse osmosis brine, *Desalination* 374 (2015) 20-30.
- [35] M. Gryta, Desalination of thermally softened water by membrane distillation process, *Desalination* 257 (2010) 30-35.
- [36] J. Phattaranawik, R. Jiraratananon, and A.G. Fane, Effects of net-type spacers on heat and mass transfer in direct contact membrane distillation and comparison with ultrafiltration studies, *J. Membr. Sci.* 217 (2003) 193-206.
- [37] H. Yu, X. Yang, R. Wang, and A.G. Fane, Numerical simulation of heat and mass transfer in direct membrane distillation in a hollow fiber module with laminar flow, *J. Membr. Sci.* 384 (2011) 107-116.
- [38] L. Martínez and J.M. Rodríguez-Maroto, On transport resistances in direct contact membrane distillation, *J. Membr. Sci.* 295 (2007) 28-39.
- [39] H. Ozbek, Viscosity of aqueous sodium chloride solutions from 0-150 °C, American Chemical Society 29th Southeast Regional Meeting, Tapa, FL, November 9-11, 1971.
- [40] L.D. Nghiem and T. Cath, A scaling mitigation approach during direct contact membrane distillation, *Sep. Purif. Technol.* 80 (2011) 315-322.
- [41] L.D. Nghiem, F. Hildinger, F.I. Hai, and T. Cath, Treatment of saline aqueous solutions using direct contact membrane distillation, *Desalin. Water Treat.* 32 (2011) 234-241.
- [42] A. Hausmann, P. Sancio, T. Vasiljevic, U. Kulozik, and M. Duke, Performance assessment of membrane distillation for skim milk and whey processing, *J. Dairy Sci.* 97 (2014) 56-71.
- [43] Y.Z. Tan, J.W. Chew, and W.B. Krantz, Effect of humic-acid fouling on membrane distillation, *J. Membr. Sci.* 504 (2016) 263-273.
- [44] J. Ge, Y. Peng, Z. Li, P. Chen, and S. Wang, Membrane fouling and wetting in a DCMD process for RO brine concentration, *Desalination* 344 (2014) 97-107.
- [45] D.M. Warsinger, J. Swaminathan, E. Guillen-Burrieza, H.A. Arafat, and J.H. Lienhard V, Scaling and fouling in membrane distillation for desalination applications: A review, *Desalination* 356 (2014) 294-313.
- [46] D.W. Green and R.H. Perry, *Perry's Chemical Engineers' Handbook*, Eighth Edition, The McGraw-Hill Companies, Inc., 2008.
- [47] D. Winter, J. Koschikowski, and M. Wieghaus, Desalination using membrane distillation: Experimental studies on full scale spiral wound modules, *J. Membr. Sci.* 375 (2011) 104-112.
- [48] E. Guillén-Burrieza, G. Zaragoza, S. Miralles-Cuevas, and J. Blanco, Experimental evaluation of two pilot-scale membrane distillation modules used for solar desalination, *J. Membr. Sci.* 409–410 (2012) 264-275.

- [49] H.C. Duong, P. Cooper, B. Nelemans, T.Y. Cath, and L.D. Nghiem, Evaluating energy consumption of membrane distillation for seawater desalination using a pilot air gap system, *Sep. Purif. Technol.* 166 (2016) 55-62.